

SHORTWAVE RADIATION FROM A VACUUM SPARK

S. V. LEBEDEV, S. L. MANDEL'SHTAM, and G. M. RODIN

P. N. Lebedev Physics Institute Academy of Sciences, U.S.S.R.

Submitted to JETP editor March 3, 1959

J. Exptl. Theoret. Phys. (U.S.S.R.) 37, 349-354 (August, 1959)

It has been established that a spectroscopic light source — a vacuum “hot” spark — emits soft x-ray radiation (wavelengths shorter than 6 Å). The radiation intensity remains quite high in the arc stage of the discharge, in which case the potential difference across the electrodes is less than 100 volts. A spectroscopic measurement of the electron temperature (Al VII line) indicates $T_e = 200,000^\circ$.

INTRODUCTION

It is well known that in the so-called “hot” vacuum spark, spectra due to highly ionized atoms are excited; in many cases these atoms lose half or more of their electrons, for example Fe XVII, Al XII, or C V. The radiation from these atoms lies in the vacuum ultraviolet and the soft x-ray regions of the spectrum. The spectra of these sparks have been investigated to 6 Å.¹ These emission spectra require energies of the order of 2000 eV in order to be excited.* Although the vacuum spark has been used for a long time in spectroscopic investigations to produce spectra of multiply charged ions the excitation mechanism is not yet understood. A first step toward this goal is the correlation of the time behavior of this radiation with the electrical characteristics of the discharge.

The present paper describes the results of an investigation of this problem in the harder radiation region with wavelengths shorter than 6 Å.

It is also of interest to estimate the temperature of the discharge by a spectroscopic method. Temperature measurements of this kind have recently been reported by Akimov and Malkov.²

METHOD

The spark was excited between two iron electrodes: one was a plate 2 mm thick with an aperture 5 mm in diameter while the other was a cylinder 4 mm in diameter. The distance from the base of the cylinder to the plate was 4 mm. The spark was observed through the aperture in the plane electrode. The pressure in the working

volume before the discharge was 1×10^{-5} mm Hg. Breakdown in the interelectrode space was realized by means of a triggering device. The current source was a 3.3- μ fd capacitor charged to 40 kv, the inductance of the circuit was 1.5 μ h, the damping resistance was 0.2 Ω , and the maximum current i was 4.8×10^4 amp. During the first half-cycle the cylindrical electrode was the anode.

The radiation from the spark was passed through a beryllium filter which absorbed completely the longwave part of the spectrum (to 6 or 7 Å). A scintillator wavelength shifter placed directly behind the filter was used to shift the radiation to the ultraviolet and visible; this converted radiation was detected by a system consisting of a FEU-25 photomultiplier and a cathode-ray oscilloscope. The photocurrent $I(t)$ was compared with the current $i(t)$ recorded by the other beam of the oscilloscope. The rated integrated sensitivity of the photomultiplier is 10 amp/lumen. The thickness of the beryllium filter was 0.25 mm, the diameter was 18 mm, the distance between the filter and the spark was 15 cm, and the distance to the input window of the photomultiplier was 10 cm. Two scintillators were used; A, tetraphenyl-butadiene in polystyrene 3 mm thick and B, a CsI(Tl) scintillator 5 mm thick.

RESULTS OF THE EXPERIMENTS

The first group of experiments was carried out with scintillator A. The photomultiplier was oriented in such a way that only the luminescent radiation from the scintillator reached it. Since this scintillator passes radiation shorter than approximately 1 Å (which did not strike the photomultiplier) without noticeable absorption, the radiation of the scintillator detected by the

*For example, in Fe XVII and Al XII the ionization potentials are 1266 and 2085 volts respectively.

photomultiplier consisted of the softer part of the radiation (1 to 6 Å). Examples of the photocurrent oscillograms obtained in this way are shown in Figs. 1a and 1b. It is apparent from these oscillograms that when the discharge is excited the radiation intensity remains sizeable for 5 to 7 microseconds.

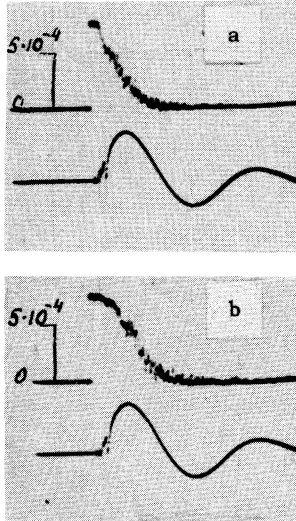


FIG. 1. Upper oscillogram: photocurrent as a function of time; this photocurrent characterizes the radiation of the vacuum spark; the lower oscillogram is the current in the spark gap. The photomultiplier is excited by the luminescence radiation of scintillator A which absorbs radiation from the spark in the region between 6 and approximately 1.5 Å. The dip at the beginning of the current curve is due to the exposure marker in the photography of the spark.

The second group of experiments was carried out with scintillator B, which absorbs completely all radiation passing through the beryllium filter. Examples of the photocurrent oscillograms obtained in this case are shown in Figs. 2a, 2b, and 2c. In the oscillograms in Figs. 2a and 2b the scintillator radiation was attenuated by six sheets of writing paper; in the oscillogram in Fig. 2c

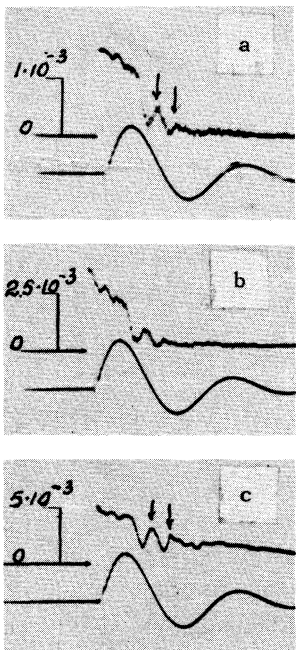


FIG. 2. The same as Fig. 1 for scintillator B, which absorbs all radiation from the spark at wavelengths shorter than 6 Å. The scintillator radiation is attenuated by six (Fig. a, b) and two (Fig. c) sheets of paper. In the last case the photomultiplier operates close to saturation. The photocurrent curves are displaced along the time axis with respect to the current curves (in Figs. 1 and 3 this displacement is much smaller).

two sheets were used. In the last case the photomultiplier was operated almost at saturation, since the light flux incident upon it was very large. Hence, at the beginning of the oscillogram in Fig. 2c the sensitivity of the photomultiplier is much smaller than in the other experiments. These measurements also indicate that the radiation lasts for a significant interval of time after breakdown — approximately 10 microseconds. The change in the radiation intensity as a function of time has a characteristic form: at a definite instant of time the radiation falls off sharply; then, near the point at which the current passes through zero, the radiation again increases, reaching a maximum at $i = 0$, then falling off and again rising, exhibiting a second maximum. In Figs. 2a, 2c, and 3b the positions of the maxima are denoted by arrows.

In a third group of experiments the photomultiplier was placed directly in the path of the beam, which passed through scintillator A; the emission of the scintillator was stopped by a filter made from black paper. The photomultiplier was excited directly by the hard radiation ($\lambda < 1$ to 1.5 Å), which was not registered in the first group of experiments and which was not separated from the

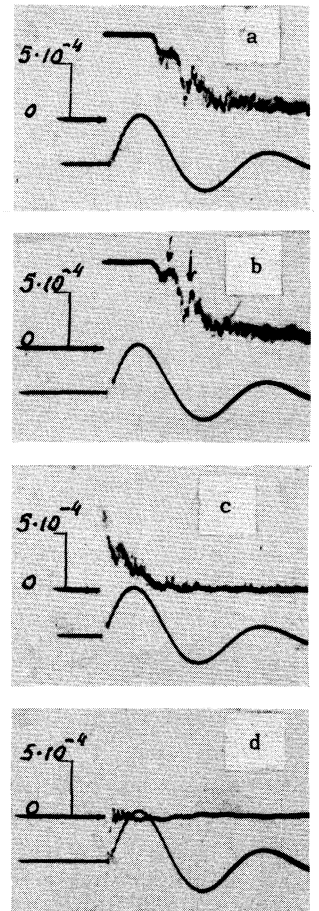


FIG. 3. The same as Fig. 1 for direct irradiation of the photomultiplier by shortwave radiation from the spark; a and b) wavelengths shorter than 1.5 Å; c) shorter than 0.6 Å; d) results of a control experiment in which a photomultiplier was covered by a copper shield 0.5 mm thick.

total radiation in the second group of experiments. The photocurrent oscillograms shown in Figs. 3a and 3b have the same characteristic features as the oscillograms of Fig. 2. The use of a supplementary filter made from nickel, 0.1 mm thick (Fig. 3c) and 0.2 mm thick leads us to the conclusion that this radiation continues to exhibit a significant intensity at least up to $\lambda = 0.6 \text{ \AA}$.

The scales for Figs. 1, 2, and 3 are apparent from the maximum value of the current, which is $4.8 \times 10^4 \text{ amp}$, and from its half-wavelength, which corresponds to a time of $7 \times 10^{-6} \text{ sec}$. The photocurrent scale is given in amperes and applies only in the oscillogram limits which have been indicated.

The results of these experiments indicate that the radiation at wavelengths between 0.6 and 6 \AA has a "post-starting" characteristic, i.e., it appears after breakdown of the gap. The results which have been observed cannot be explained by the "stretching" of the scintillator radiation. In the first group of experiments the scintillator was characterized by an emission time of less than 10^{-8} sec . However the rate of decay of the photocurrent on the oscillograms in Figs. 1a and b is considerably smaller — a reduction of the photocurrent by a factor of e (in the linear region of amplifier operation) corresponds to a time of approximately $1 \times 10^{-6} \text{ sec}$. Scintillator B, used in the second group of experiments, had an emission time of $1 \times 10^{-6} \text{ sec}$; however the shape of the photocurrent curve observed in these experiments (the existence of two maxima) again indicates that the effect cannot be explained by "stretching" of the scintillator radiation.

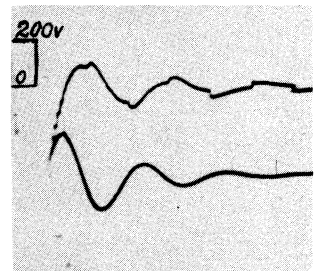
In all experiments the time delay in the oscilloscope amplifier and cable was less than $7 \times 10^{-8} \text{ sec}$. Consequently no element in the detection system could delay the signal by a time of the order of a microsecond.

To insure that the results were not due to spurious effects, the photomultiplier was shielded by black paper in the first and second groups of experiments; in the third group a copper foil was used. The photocurrent oscillograms obtained under these conditions are shown in Fig. 3d. It should be noted that each experiment was repeated at least 10 times and that the characteristic features were reproduced in all cases (Figs. 3a and 3b). The maximum spread in the photocurrent can be ascertained by a comparison of Figs. 1a and 1b. This spread is due to the fact that the luminous spot on the electrodes does not remain fixed; this was verified by photographing the electrodes in the visible region of the spectrum with an exposure time of 0.3 microseconds. Thus,

the presence of soft x-rays, which continues in the post-breakdown stage of the discharge, has been established rather reliably.

Measurements were also made to enable us to estimate the voltage drop across the interelectrode space in the stage of the discharge being discussed here. The discharge circuit described above was used for this purpose but the initial condenser voltage was reduced to 22 kv and the length of the spark gap was reduced to 2 mm. The electrodes in this case were iron and copper rods 5 mm in diameter. A lead-out section was sealed to the system at a distance of 0.5 mm from the ends of the electrodes and connected to the oscilloscope through a voltage divider (the resistance of the divider was $1 \times 10^4 \Omega$, the input capacity of the oscilloscope was $3 \times 10^{-5} \mu\text{fd}$). The oscilloscope records the sum $U = U_d + U_d^{\text{ind}} + U_0^{\text{ind}}$ where $U_d + U_d^{\text{ind}}$ is the voltage across the discharge channel (averaged over the cross section) and U_0^{ind} is the voltage across the output section and divider induced by the current i . The $U(t)$ oscillogram is shown in Fig. 4. The $U'(t) \sim di/dt$ patterns were obtained by moving the electrodes

FIG. 4. The upper oscillogram is the total voltage along the inter-electrode gap and the measurement circuit, $U(t)$. The maximum current value in the spark (lower oscillogram) is $2.5 \times 10^4 \text{ amp}$ and the half-wavelength corresponds to a time of $7 \times 10^{-6} \text{ sec}$.



together until contact was made; these differ from $U(t)$ by the absence of discontinuities at the point at which the current (i) passes through zero (the difference in the corresponding values of U and U' is close to the value of the discontinuity). From this it is apparent that the part of the detected total voltage $U(t)$ proportional to di/dt is determined basically by the voltage U_0^{ind} and that U_d^{ind} has almost no effect on the shape of the oscillogram. Consequently U_d^{ind} is much smaller than U_0^{ind} . According to Fig. 4 the maximum value of $U(t)$ is approximately 100 volts; hence the factor U_d^{ind} is not more than several tens of volts. The other part of the voltage drop in the interelectrode space U_d is not due to the inductance and is clearly expressed at the end of the $U(t)$ oscillogram where $U_d^{\text{ind}} + U_0^{\text{ind}}$ become small because the current i is reduced. $U_d(t)$ exhibits approximately the same nature and magnitude (approximately 20 volts) as the voltage drop across a gap in air, which has been studied in detail at lower currents.

Wave-length A	Transition	Energy of the upper level, ev	AiGi, sec ⁻¹
240.77	$2p^3 \ ^2D_{3/2}^0 - 2p^4 \ ^2P_{3/2}$	59	$1.14 \cdot 10^{11}$
356.885	$2p^3 \ ^4S_{3/2}^0 - 2p^4 \ ^4P_{3/2}$	35	$0.63 \cdot 10^{11}$

Thus, the total voltage drop in the vacuum spark $U_d + U_d^{\text{ind}}$ amounts to tens of volts and, in any case, is never greater than 100 volts. However we may note that at higher currents and frequencies U_d^{ind} increases in proportion to di/dt .

In principle the connection between the first maximum on the photocurrent oscillograms in Fig. 2 and the possible significant increase in the voltage between the electrodes at the moment the current in the spark passes through zero is not unusual; this phenomenon is well known for air discharges. However we do not see the voltage discontinuities in our oscillograms; hence if they appear in the vacuum spark their duration is less than 3×10^{-7} sec. It should also be noted that voltage discontinuities cannot explain the second maximum in the photocurrent oscillograms.

ESTIMATE OF THE TEMPERATURE OF A VACUUM SPARK

The temperature of a vacuum spark was determined by the Ornshtein technique, using the intensities of the Al VII lines. The transition probabilities for these lines were computed in the Coulomb approximation using the Bates and Damgaard technique. The wavelengths, spectroscopic notation, upper level energies, and transition probabilities (AiGi) are given in the table.

In these measurements the maximum current in the spark was 1.3×10^4 amp and the circuit inductance was $2.6 \mu\text{h}$. The spark was produced by a $1\text{-}\mu\text{fd}$ capacitor charged to 24 kv. These spectra were obtained with a vacuum spectrograph (DFS-6) with a diffraction grating in the oblique incidence unit. The spectrum was photographed on a film which was sensitized by a solution of sodium salicylate in methyl alcohol. The measurements of the relative intensities of the spectral lines were carried out in the first and second order spectra under the assumption that the quantum yield of the luminescent radiation of the sodium salicylate is constant. Intensity markers were obtained by means of a stepped quartz absorber at a wavelength close to the maximum of the radiation of the sensitizer.

The value of the electron temperature in the vacuum spark was found to be of the order of 2×10^5 °K.

It should be noted that although the heterochromatic photometry technique which we have used is standard in the vacuum region of the spectrum³ the constancy of the quantum yield of the sensitizer used by us has been checked only up to 700 Å.^{4,5} Hence it is possible that the use of this method in the shorter wavelength region may lead to errors which we are not able to evaluate at the present time.

The measured value of the temperature is in good agreement with an estimate made from the general form of the spectrum. An analysis of the spectrogram indicates that for the conditions at hand the Al VI and Al VII lines are intense, the Al VIII line is weak and the Al IX and Al X lines are invisible. In Fig. 5 is shown the line intensity for these ions, as a function of temperature, computed from the Saha-Boltzmann formula for the lines with the highest intensities with excitation potentials of 30–40 volts for electron concentrations* $n_e = 10^{18}$ electrons/cm³.

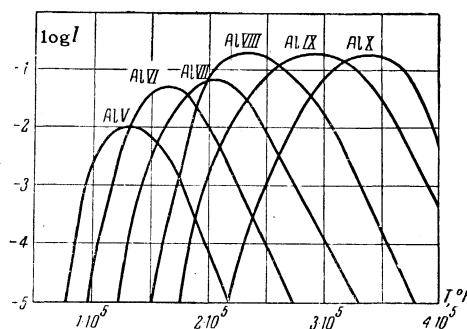


FIG. 5. Intensity of the lines of multiply charged ions as a function of temperature computed from the Saha-Boltzmann formula for $n_e = 10^{18}$ electron/cm³.

It is apparent from this figure that the observed shape of the spectrum corresponds to a temperature $T = 1.8 \times 10^5$ °K. When $n_e = 10^{17}$ and $n_e = 10^{19}$ electrons/cm³ the intensities of the Al VI and Al VII lines become equal to $T = 1.5 \times 10^5$ and $T = 2.1 \times 10^5$ °K; all of these values are in good

*The quantity n_e is estimated from the conductivity of the discharge on the basis of the current measurements, the measurements of the voltage drops between electrodes, and the diameter of the discharge channel (the channel was photographed in the visible region with a Kerr cell). Values of n_e between 10^{17} and 10^{19} electrons/cm³ were obtained.

agreement with the results of the present temperature measurements $T_e = 2 \times 10^5$ °K and are much higher than the value $T \approx 4.6 \times 10^4$ °K obtained by Akimov and Malkov² using the Al III lines. As has been noted by these authors, the temperature values they report correspond to the instant at which the ions are excited. It is probable that this given temperature characterizes the peripheral (colder) portions or later stages of the discharge.

CONCLUSION

We have observed shortwave radiation which, to a considerable degree, is not "starting" radiation and which is to be associated with the later stages of the discharge; it is probable that this radiation is due to the radiation of the plasma itself — the ion line and continuous spectra. However the possibility is not excluded that the radiation is due to electron bremsstrahlung at the electrodes. Before this problem can be solved the radiation will have to be examined by means of spectral analyses.

The energy of the corresponding photons is 2×10^3 to 2×10^4 eV; thus, this radiation cannot be attributed to electrons which are directly accelerated by the voltage between the electrodes since this voltage is less than 100 volts. Moreover, the observed radiation cannot be explained by "thermal" electrons because at a temperature of 20 eV the number of electrons with energies between 2×10^3 and 2×10^4 eV is clearly not sufficient to produce the sizeable intensity which is observed. Thus we are forced to assume that

the mechanism by which this radiation is produced is analogous to the mechanism responsible for the hard radiation in high-intensity pulsed discharges, such as those which have been observed in recent years;^{6,7} this mechanism is still not fully understood. The problem will require further investigation and is under study at the present time. It seems to us that one of the probable origins for this effect may be the production, in localized regions of the plasma, of high-intensity electric fields, which are induced as a consequence of its deformation.⁸

¹ B. Edlen, *Physica*, **13**, 545 (1947).

² E. M. Akimov and I. P. Malkov, *Оптика и спектроскопия (Optics and Spectroscopy)* **6**, 96 (1959).

³ H. Greiner, *Z. Naturforsch.* **12**, 735 (1957).

⁴ Herman-Montagne, Lewi, and Ricard, *Compt. rend.*, **202**, 1668 (1936).

⁵ Johnson, Watanabe, and Tousey, *J. Opt. Soc. Am.* **41**, 702 (1951).

⁶ S. Yu. Luk'yanov and I. M. Podgornyĭ, *Атомная энергия (Atomic Energy)* **3**, 97 (1956).

⁷ Podgornyĭ, Kovalevskii, and Pal'chikov, *Dokl. Akad. Nauk SSSR* **123**, 825 (1958), *Soviet Phys. Doklady* **3**, 1208 (1959).

⁸ B. A. Trubnikov, *Физика плазмы и проблема управляемых термоядерных реакций (Plasma Physics and the Problem of a Controlled Thermonuclear Reaction)* U.S.S.R. Acad. Sci. 1958, Vol. 4, p. 87.

Translated by H. Lashinsky